EXPLORING OPTIMAL WORKING FLUIDS AND CYCLE ARCHITECTURES FOR ORGANIC RANKINE CYCLE SYSTEMS USING ADVANCED COMPUTER-AIDED MOLECULAR DESIGN METHODOLOGIES

White M.T., Oyewunmi O.A., Haslam, A.J. and Markides C.N.*
* Author for correspondence:
Clean Energy Processes (CEP) Laboratory,
Department of Chemical Engineering,
Imperial College London,
South Kensington Campus,
London SW7 2AZ, UK,
E-mail: c.markides@imperial.ac.uk

ABSTRACT

The combination of computer-aided molecular design (CAMD) with an organic Rankine cycle (ORC) power-system model presents a powerful methodology that facilitates an integrated approach to simultaneous working-fluid design and power-system thermodynamic or thermoeconomic optimisation. Existing CAMD-ORC models have been focussed on simple subcritical, non-recuperated ORC systems. The current work introduces partially evaporated or trilateral cycles, recuperated cycles and working-fluid mixtures into the ORC power-system model, which to the best knowledge of the authors has not been previously attempted. A necessary feature of a CAMD-ORC model is the use of a mixed-integer non-linear programming (MINLP) optimiser to simultaneously optimise integer working-fluid variables and continuous thermodynamic cycle and economic variables. In this paper, this feature is exploited by introducing binary optimisation variables to describe the cycle layout, thus enabling the cycle architecture to be optimised alongside the working fluid and system conditions. After describing the models for the alternative cycles, the optimisation problem is completed for a defined heat source, considering hydrocarbon working fluids. Two specific case studies are considered, in which the power output from the ORC system is maximised. These differ in the treatment of the minimum heat-source outlet temperature, which is unconstrained in the first case study, but constrained in the second. This is done to replicate scenarios such as a combined heat and power (CHP) plant, or applications where condensation of the waste-heat stream must be avoided. In both cases it is found that a working-fluid mixture can perform better than a pure working fluid. Furthermore, it is found that partially-evaporated and recuperated cycles are optimal for the unconstrained and constrained case studies respectively.

NOMENCLATURE

c_{p}	[J/(kg K)]	specific heat capacity
P_2	[Pa]	evaporation pressure
P_{cr}	[Pa]	critical pressure
P_{r}	[-]	reduced pressure
$PP_{\mathrm{c}}, PP_{\mathrm{h}}$	[K]	condenser and evaporator pinch points
T_1	[K]	condensation temperature
$T_{3'}$	[K]	saturated-vapour temperature
$T_{\mathrm{hi}}, T_{\mathrm{ci}}$	[K]	heat-source and heat-sink inlet temperatures
x	[-]	mass fraction
z	[-]	superheating parameter
$\eta_{\mathrm{p}}, \eta_{\mathrm{e}}$	[-]	pump and expander isentropic efficiencies
ϵ_{r}	[-]	recuperator effectiveness
$\dot{m}$	[kg/s]	mass flow rate
$\dot{W}_{\mathrm{n}}$	[W]	net power output
ΔT_{sh}	[K]	amount of superheating

INTRODUCTION

The organic Rankine cycle (ORC) is a very promising technology for the conversion of low- and medium-grade heat from solar, geothermal and industrial processes into power [1]. However, the identification the optimal working fluids, and cycle architectures that maximise either the thermodynamic or technoeconomic performance of a system for a targeted application, remain pertinent questions to be addressed by research.

A novel approach to working-fluid selection is the introduction of computer-aided molecular-design (CAMD) to simultaneously optimise the molecular structure of the working fluid and the thermodynamic system in a single design framework. This is facilitated by using a group-contribution equation of state. A number of studies have coupled empirical group-contribution equations of state with an ORC process model and demonstrated the potential of the method to identify new working fluids [2; 3]. More advanced equations of state have also been applied [4], and a fully integrated CAMD-ORC model has been used to identify optimal working fluids for a specific application [5]. Furthermore, the authors of this current paper have also recently developed a similar CAMD-ORC model [6], based on the advanced SAFT-γ Mie equation of state [7], and have integrated group-contribution transport-property prediction methods to facilitate the sizing of the system components.

In terms of novel cycle architectures, the use of working-fluid mixtures results in non-isothermal isobaric phase change

processes, which leads to a better thermal match between the working fluid and heat source, and can lead to improved thermodynamic performance [8; 9]. Furthermore, the introduction of a partially-evaporated cycle, in which expansion occurs from a two-phase state, can also be used to increase the power output from the system [10]. A temperature–entropy diagram of these two cycles is provided in Figure 1. However, to the authors' knowledge, the CAMD-ORC models that have been developed so far have focussed on subcritical, superheated ORC systems.

The aim of the current paper is to introduce models for novel cycle architectures, including partially-evaporated and recuperated cycles, and cycles operating with mixtures into the CAMD-ORC framework. This allows these novel cycle architectures to be considered within the MINLP optimisation problem, facilitating the identification of not only the optimal working fluid for a particular application, but also the optimal cycle architecture.

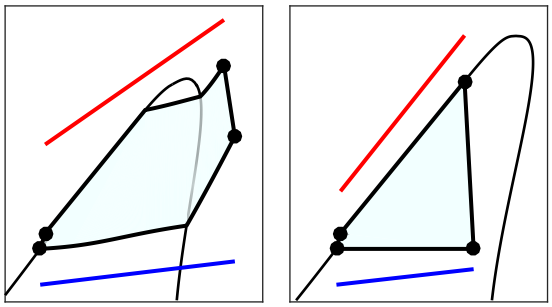

Figure 1. A representative T-s diagram of a basic ORC operating with a mixture (left) and a partially-evaporated ORC (right).

CAMD-ORC MODEL

Thermophysical property prediction

Group-contribution methods determine the properties of a particular molecule based on the functional groups of which it is composed. For example, n-pentane is described by two –CH_3 groups and three >CH_2 groups, whilst isopentane is described by three –CH_3 groups, one >CH_2 and one >CH– group. In a group-contribution method group parameters are required only for the individual groups. It is this feature that makes CAMD possible by allowing the evaluation of novel working fluids for which property prediction would not be possible using conventional approaches. In this work, the SAFT-γ Mie equation of state [7] is used for thermodynamic property prediction. SAFT-γ Mie a state-of-the-art version of statistical associating fluid theory (SAFT) [11; 12] wherein a Mie potential is used to model the interaction between two molecular groups [7]. Group-contribution parameters are available for the hydrocarbon groups considered within this paper, and have been validated against experimental data [13].

Thermodynamic modelling

The thermodynamic analysis of the ORC is well described within the literature, and consists of applying an energy balance to each component with the cycle. The main thermodynamic variables that are used to describe the ORC in this work are the condensation temperature T_1, the reduced evaporation pressure P_r (P_2/P_cr, where P_2 and P_cr are the evaporation and critical pressures respectively), and a superheating parameter z, which can vary between 0 and 2. The introduction of this parameter allows the consideration of both superheated and partially-evaporated ORCs within the same model. When $0 \leq z \leq 1$, the working fluid is assumed to expand from a two-phase state and z is equal to the expander inlet vapour quality. However, when $1 < z \leq 2$ the working fluid expands from a superheated state and the amount of superheating ΔT_sh is given by:

$$\Delta T_\mathrm{sh} = (z-1)(T_\mathrm{hi} - T_{3'})\,, \tag{1}$$

where T_hi is the heat-source inlet temperature and $T_{3'}$ is the saturated-vapour temperature.

Alongside these three parameters, the pump and expander are modelled by assuming fixed isentropic efficiencies, denoted η_p and η_e respectively, and the minimum allowable evaporator and condenser pinch points are also defined, denoted $PP_\mathrm{h,min}$ and $PP_\mathrm{c,min}$ respectively. It is noted that when $z = 2$, $T_\mathrm{hi} = T_{3'}$ which is a violation of the imposed evaporator pinch point. Therefore, within an optimisation the pinch constraint ($T_\mathrm{hi} - T_{3'} > PP_\mathrm{h,min}$) will always result in cycles where $z < 2$. Finally, in the case of a recuperated cycle, the recuperator effectiveness ϵ_r is also defined, whilst for a working-fluid mixture both working fluids are described in terms of their functional groups, and the variable x represents the mass fraction of Fluid 1, the first mentioned fluid in each pairing.

MODEL VALIDATION

The CAMD-ORC model has previously been validated against NIST REFPROP for a non-recuperated, sub-critical ORC operating with various hydrocarbon working fluids [6]. In this section this validation study will be repeated for the alternative cycle architectures considered within this paper. Although the model is expected to be applicable for the range of heat-source temperatures relevant to ORC systems (i.e., 373–673 K), for the validation study the heat source is assumed to be at 473 K. The thermodynamic performance of an ORC system is independent of the heat-source mass-flow rate and therefore the heat-source is defined with a heat-capacity rate of $\dot{m}c_\mathrm{p} = 4.2$ kW/K. Finally, $\eta_\mathrm{p} = 0.7$, $\eta_\mathrm{e} = 0.8$, $T_1 = 303$ K and $PP_\mathrm{h,min} = 10$ K are assumed, which are representative of a typical ORC system.

Partially-evaporated cycles

For the validation of the partially-evaporated cycle model three different working fluids have been considered, namely n-pentane, n-hexane and isopentane. For these three fluids a parametric study was completed in which z was varied between 0 and 2, and this was repeated at different evaporation pressures. The comparison between the results obtained using the CAMD-ORC model, based on SAFT-γ Mie, and a similar model using NIST REFPROP is given in Figure 2.

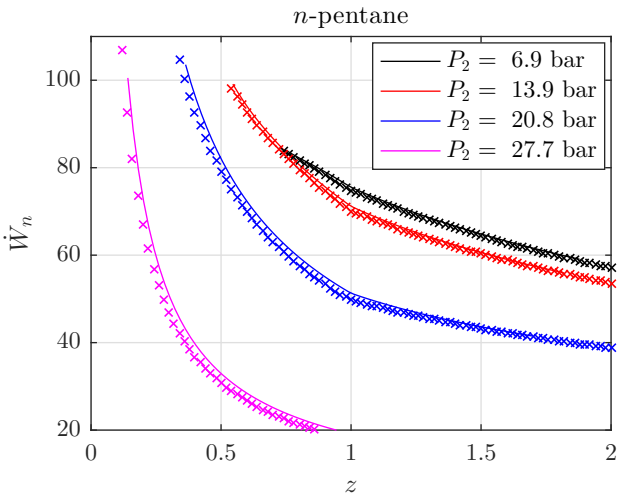

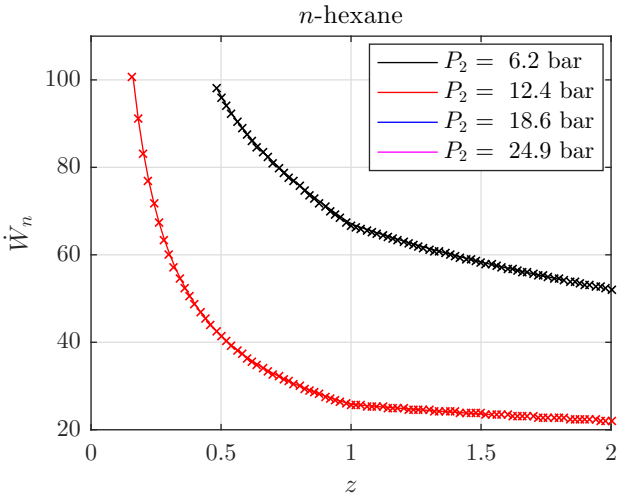

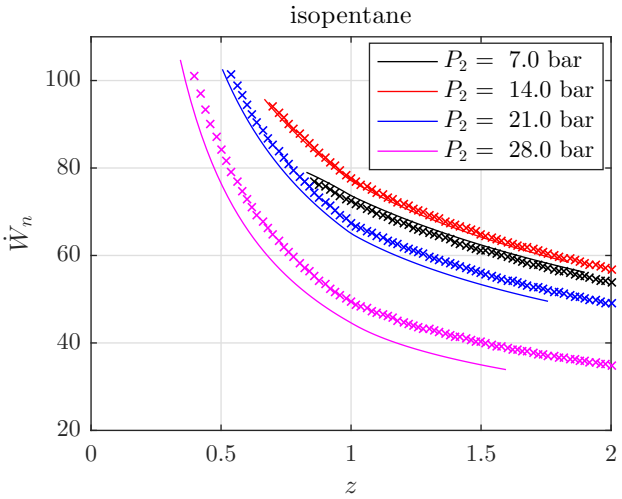

Figure 2. Comparison between the power output ($\dot{W}_\mathrm{n}$ in kW) predicted by the CAMD-ORC model ($\times$ markers) and NIST REFPROP (continuous curves) for three different working fluids operating within a partially-evaporated ($z < 1$) and a superheated ($z \geq 1$) cycle.

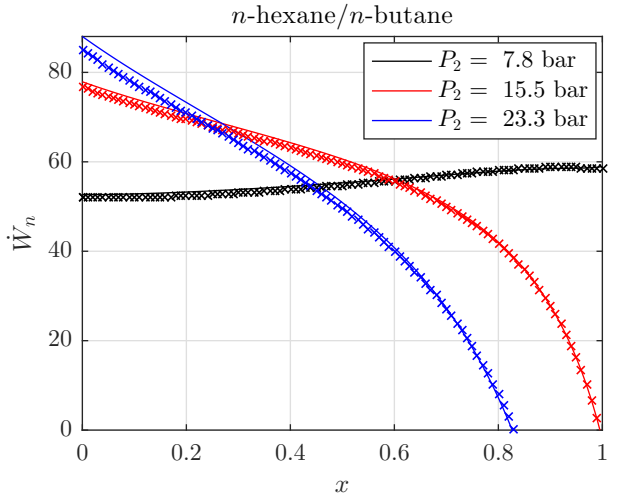

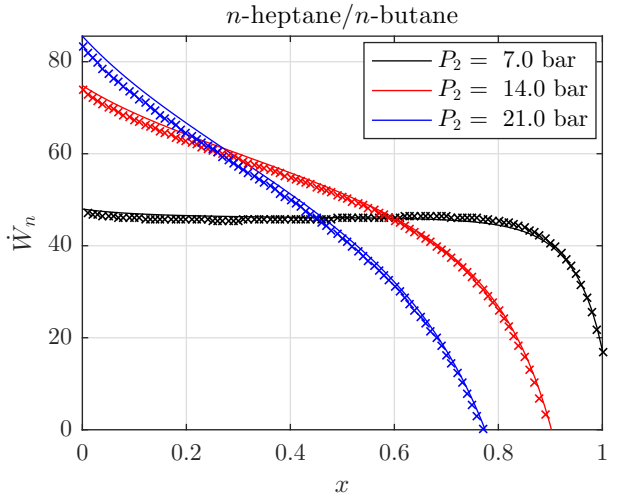

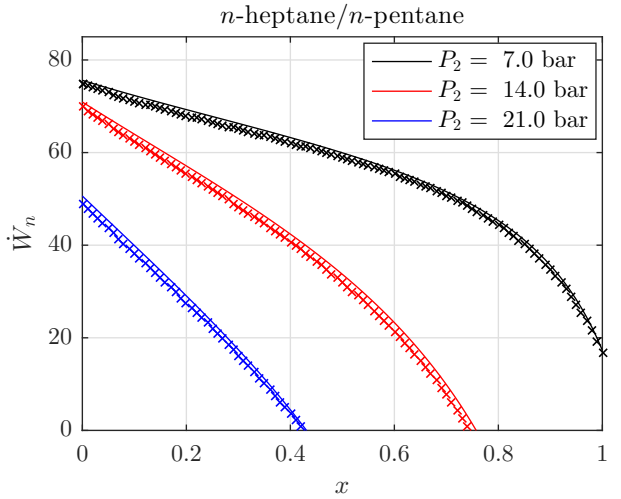

Figure 3. Comparison between the power output ($\dot{W}_\mathrm{n}$ in kW) predicted by the CAMD-ORC model ($\times$ markers) and NIST REFPROP (continuous curves) for three different fluid mixtures.

Overall, it is observed that, except for the 28.0 bar case for isopentane, a very good agreement between the two models is obtained and this validates the suitability of the CAMD-ORC model to simulate these types of cycles. The deviation for the 28.0 bar isopentane case can be explained because at higher pressures the cycle is operating closer to the critical point (33.8 bar), and the deviation between SAFT-γ Mie and NIST REFPROP is found to increase as the critical point is approached. The 18.6 and 24.9 bar cases for n-hexane do not appear in Figure 2 because the saturation temperature of n-hexane at these pressures is higher than the heat-source temperature.

More generally, from Figure 2 it is observed that the maximum power is always generated when $z < 1$, which clearly indicates the potential thermodynamic performance benefit of allowing the working fluid to expand from a two-phase state.

Mixtures

For the validation of the CAMD-ORC model for mixtures, three different mixtures have been considered, namely n-hexane/n-butane, n-heptane/n-butane and n-heptane/n-pentane. For each mixture a parametric study was completed in which the mass fraction of Fluid 1, x, was varied from 0 to 1, and this was repeated at different evaporation pressures. In each case, it was assumed that expansion occurs from a saturated-vapour state (i.e., $z = 1$). The comparison between the results obtained using the CAMD-ORC model, and the model based on NIST REFPROP is shown in Figure 3. Again, a very good agreement is observed for the different case studies, thus validating the CAMD-ORC model for simulating these types of cycles as well.

CASE STUDY

The CAMD-ORC framework can now be applied to the optimisation of an ORC system for a particular application. For this we consider a geothermal case study discussed within the literature [14], in which the heat source is used to generate electricity and supply heat to a district-heating network. Within our study we optimise the power output from the system under two conditions. The first constrains the heat-source outlet temperature to the temperature required by the district-heating network (353 K), whilst the second represents the case when there is no heating demand and the heat-source outlet temperature is unconstrained. Under both operating conditions the aim is to find the optimal cycle architecture and working fluid. The assumptions for the study are listed in Table 1.

The fluids under consideration are both pure fluids and working-fluid mixtures from the normal alkane family (*i.e.*, n-propane, n-butane, n-pentane *etc.*), which are described by two –CH_3 groups and a variable number of $>CH_2$ groups. Therefore the variables being considered within the optimisation include variables describing the working fluid, the cycle architecture, and operating conditions, and these are summarised in Table 2. There are continuous, integer and binary variables and therefore the optimisation is of the mixed-integer non-linear programming (MINLP) type. The minimum allowable evaporator and condenser pinch points are set to $PP_{\mathrm{h,min}} = 10$ K and $PP_{\mathrm{c,min}} = 5$ K respectively. In the case of a working-fluid mixture, the mass fraction is constrained to not allow mixtures when the mass fraction of one of the fluids is less than 2.5%. Furthermore, the superheating parameter is constrained to $z > 0.05$ to avoid expansion directly from a saturated-liquid state.

Table 1. Assumptions for the case study.

Brine inlet temperature [14]	T_{hi}	397	K
Brine outlet temperature (CHP) [14]	T_{ho}	353	K
Brine specific-heat capacity	$c_{\mathrm{p,h}}$	4030	J/(kg K)
Brine mass-flow rate [14]	$\dot{m}_{\mathrm{h}}$	90	kg/s
Cooling-water inlet temperature [14]	T_{ci}	278	K
Cooling-water specific-heat capacity	$c_{\mathrm{p,c}}$	4200	J/(kg K)
Cooling-water mass-flow rate [14]	$\dot{m}_{\mathrm{c}}$	182	kg/s
Pump isentropic efficiency	η_{p}	0.7	-
Expander isentropic efficiency	η_{e}	0.8	-
Recuperator effectiveness	ϵ_{r}	0.7	-

Table 2. Optimisation variables.

Variable		Type	Limits
Condensation temperature	T_1	Continuous	278–353 K
Reduced pressure	P_{r}	Continuous	0.001–0.85
Superheating parameter	z	Continuous	0.05–2
Evaporator pinch point	PP_{h}	Continuous	10–100 K
Composition of Fluid 1	x	Continuous	0.025–0.975
Number of $>CH_2$ groups (Fluid 1)	-	Integer	1–6
Number of $>CH_2$ groups (Fluid 2)	-	Integer	1–6
Recuperator flag	-	Binary	0–1

RESULTS AND DISCUSSION

Considering the constrained heat-source outlet temperature case study, the MINLP optimisation was completed and in a single optimisation process the CAMD-ORC framework was able to identify an optimal working fluid and cycle architecture to maximise the power output. In order to verify that the cycle obtained from the MINLP optimisation is the optimal configuration a number of simpler optimisation studies were completed. These studies removed the integer and binary variables, therefore fixing the working fluid and the decision to include a recuperator, which simplifies the optimisation to non-linear programming (NLP) optimisation in which only the continuous variables (*i.e.*, T_1, P_{r}, z, PP_{h} and x) are optimised. The results obtained for the MINLP and NLP optimisations are shown in Figure 4. It should be noted that because recuperation is not possible for a partially-evaporated cycle, the model ignores the recuperator flag if a partially-evaporated cycle is being considered within the optimisation. This explains why the two optimisations for n-pentane and n-hexane both converge on the same optimal cycle.

Overall, the results shown in Figure 4 are very promising, with the MINLP optimisation correctly identfying the optimal working fluid and cycle architecture that results in the highest power output from the system. In this instance, the optimal cycle is a superheated ($z > 1$), recuperated cycle operating with a mixture composed from n-butane (96%) and n-heptane (4%). The resulting net power output from the system is 2.32 MW.

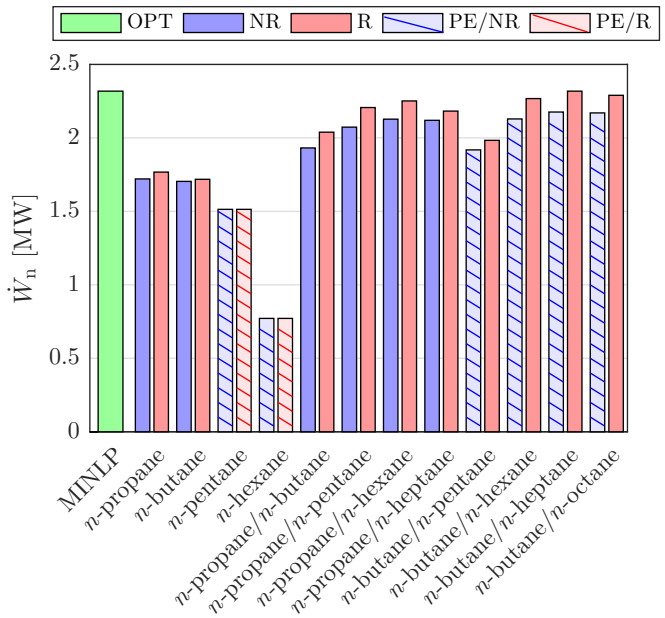

Figure 4. Comparison between the optimal cycles identified from the MINLP (OPT) and NLP optimisations for the constrained heat-source outlet temperature. The different bars correspond to: superheated with recuperator flag set to 0 (NR); superheated with recuperator flag set to 1 (R); partially-evaporated with recuperator flag set to 0 (PE/NR); partially-evaporated with recuperator flag set to 1 (PE/R).

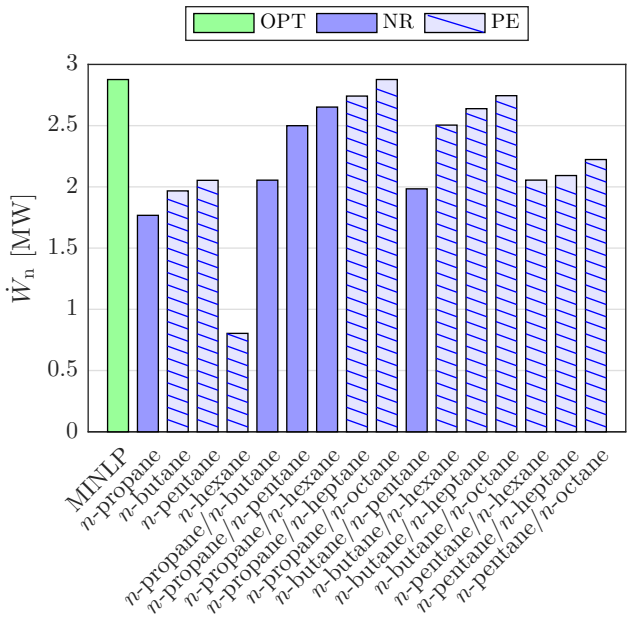

Figure 5. Comparison between the optimal cycles identified from the MINLP (OPT) and NLP optimisations for the unconstrained heat-source outlet temperature. The different cycle architectures are identified as non-recuperated (NR) and partially-evaporated (PE). In all cases the recuperator flag is set to 0.

In addition to verifying the MINLP optimisation, the NLP optimisation studies also provide insights into cycle selection. In the case of a constrained heat-source outlet temperature a recuperator will generally lead to a higher power output. Furthermore, for some of the working-fluid mixtures investigated the choice of whether or not a recuperator is installed can affect the resulting cycle architecture. For example, for the mixtures on the right-hand side of Figure 4, using a recuperator results in a superheated cycle. However, if it is not possible to install a recuperator, perhaps due to increased investment costs or increased complexity, operating a partially-evaporated could have thermodynamic benefits. Finally, it is noted that a clear improvement in thermodynamic performance is observed when using a mixture compared to using a pure fluid. Furthermore, as the difference in the chain length of the two working fluids that make up the mixture increases, the power output from the system increases.

Considering the unconstrained case study a similar comparison between MINLP and NLP optimisation studies has been completed. The results are presented in Figure 5. As with the constrained case study, the results for the unconstrained heat-source are also promising with the MINLP optimisation identifying the optimal cycle architecture that maximises the power output. In this instance a maximum net power of 2.88 MW is obtained when operating a partially-evaporated cycle ($z = 0.36$), with a mixture of n-propane (96%) and n-octane (4%).

In terms of the results for the NLP optimisations, it is again observed that using a working-fluid mixture generally results in a higher power output from the system compared to using a pure fluid, and the power output from a cycle operating with a mixture increases as the difference in the chain length of the two working fluids increases. Furthermore, the NLP optimisations that result in the higher power outputs are also partially-evaporated cycles. Therefore, since the working fluid is in a two-phase state at the expander outlet it is not possible to install a recuperator, and as a result it is not necessary to consider recuperated cycles when the heat-source outlet temperature is unconstrained.

In Figure 6, the optimal cycles for the constrained and unconstrained heat-source outlet temperature case studies are shown. It is clear that the two different cases result in significantly different cycles. However, in both cases, the improved temperature profiles within the heat exchangers that result from using a mixture are apparent, particularly within the condenser. However, the authors note that using mixtures can lead to heat-transfer degradation [15], which could mitigate the improved thermodynamic performance. This trade-off should be the focus of future research. It is also observed that the unconstrained case study has a lower heat-source outlet temperature, which in turn results in the ORC extracting more heat from the heat source. Ultimately, constraining the heat-source outlet temperature reduces the power output from the system by 19%. Of course, for the case study under consideration, the heat source leaving the evaporator is not wasted since it is used for district heating. Therefore there exists a trade-off between power output and heat-source outlet temperature which affects the cycle architecture that should be selected.

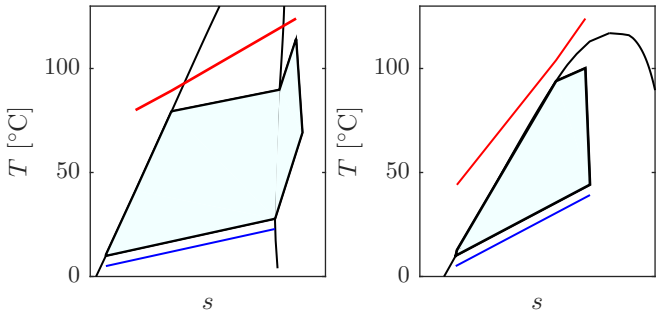

Figure 6. The optimal cycles for the constrained (left) and unconstrained (right) heat-source temperature. The red and blue lines are heat-source and heat-sink profiles respectively, and the shaded area enclosed by the black lines is the ORC.

CONCLUSION

We have extended an existing CAMD-ORC framework to allow the consideration of novel cycle architectures including recuperated and partially-evaporated cycles, and cycles operating with working-fluid mixtures. The framework is capable of simultaneously optimising the molecular structure of the working fluid, the cycle architecture and the cycle operating parameters in a single optimisation. After validating the thermodynamic model against NIST REFPROP, the CAMD-ORC framework was applied to a case study in which the power output from the system is maximised under two operating conditions, corresponding to a constrained and unconstrained heat-source outlet temperature respectively. In both cases, it is found that the CAMD-ORC framework can accurately identify the optimal cycle architecture and working fluid. For the constrained case study a superheated, non-recuperated cycle operating with a mixture of 96% n-butane/4% n-heptane results in an optimal power output of 2.32 MW. An unconstrained cycle results in a 25% increase in power output, corresponding to 2.88 MW, and is obtained for a partially-evaporated cycle operating with a mixture of 96% n-propane/4% n-octane. More generally, it is observed that a recuperated cycle can be beneficial for improving the power output from the system when the heat-source outlet temperature is constrained, whilst partially-evaporated cycles are the best choice when the heat-source outlet temperature is unconstrained. Therefore the cycle architecture is strongly dependent on the heat source. Furthermore, it is found that mixtures result in higher power outputs than using pure fluids, and the maximum power output increases as the difference in the chain length of the two fluids increases.

ACKNOWLEDGMENT

This work was supported by the UK Engineering and Physical Sciences Research Council (EPSRC) [grant number EP/P004709/1]. Data supporting this publication can be obtained on request from cep-lab@imperial.ac.uk.

REFERENCES

[1] Markides, C.N., Low-concentration solar-power systems based on organic Rankine cycles for distributed-scale applications: Overview and further developments, *Frontiers in Energy Research*, Vol. 3, No. 12, 2015, pp. 1-16.

[2] Papadopoulos, A.I., Stijepovic, M., and Linke, P., On the systematic design and selection of optimal working fluids for organic Rankine cycles, *Applied Thermal Engineering*, Vol. 30, No. 6-7, 2010, pp. 760-769.

[3] Palma-Flores, O., Flores-Tlacuahuac, A., and Canseco-Melchorb, G, Simultaneous molecular and process design for waste heat recovery, *Energy*, Vol. 99, 2016, pp. 32-47.

[4] Lampe, M., Stavrou, M., Schilling, J., Sauer, E., Gross, J., and Bardow, A., Computer-aided molecular design in the continuous-molecular targeting framework using group-contribution PC-SAFT, *Computers and Chemical Engineering*, Vol. 81, 2015, pp. 278-287.

[5] Schilling, J., Lampe, M., Gross, J. and Bardow, A., 1-stage CoMT-CAMD: An approach for integrated design of ORC process and working fluid using PC-SAFT, *Chemical Engineering Science*, Vol. 159, 2017, pp. 217-230.

[6] White, M.T., Oyewunmi, O.A., Haslam, A.J., and Markides, C.N., Industrial waste-heat recovery through integrated computer-aided working-fluid and ORC system optimisation using SAFT-γ Mie, *Energy Conversion and Management*, Accepted manuscript.

[7] Papaioannou, V., Lafitte, T., Avendaño, C., Adjiman, C.S., Jackson, G., Müller, E.A., and Galindo, A., Group contribution methodology based on the statistical associating fluid theory for heteronuclear moleculrs formed from Mie segments, *Journal of Chemical Physics*, Vol. 140, No. 5, 2014, pp. 1-29.

[8] Lecompte, S., Ameel, B., Ziviani, D., Van Den Broek, M., and De Paepe, M., Exergy analysis of zeotropic mixtures as working fluids in organic Rankine cycles, *Energy Conversion and Management*, Vol. 85, 2014, pp. 727-739.

[9] Oyewunmi, O.A., Taleb, A.I., Haslam, A.J., and Markides, C.N., On the use of SAFT-VR Mie for assessing large-glide fluorocarbon working-fluid mixtures in organic Rankine cycles, *Applied Energy*, Vol. 163, 2016, pp. 263-282.

[10] Fischer, J., Comparison of trilateral cycles and organic Rankine cycles, *Energy*, Vol. 36, No. 10, 2011, pp. 6208-6219.

[11] Chapman, W.G., Gubbins, K.E., Jackson, G., and Radosz, M., SAFT: Equation-of-state solution model for associating fluids, *Fluid Phase Equilibria*, Vol. 52, 1989, pp. 31-38.

[12] Chapman W.G., Gubbins K.E., Jackson, G., and Radosz, R., New reference equation of state for associating fluids, *Industrial & Engineering Chemistry Research*, Vol. 29, No. 8, 1990, pp. 1709-1721.

[13] Dufal, S., Papaioannou, V., Sadeqzadeh, M., Pogiatzis, T., Chremos, A., Adjiman, C.S., Jackson, G., and Galindo, A., Prediction of thermodynamic properties and phase behaviour of fluids and mixtures with the SAFT-γ Mie group-contribution equation of state, *Journal of Chemical and Engineering Data*, Vol. 59, No. 10, 2014, pp. 3272-3288.

[14] DiPippo, R., Second law assessment of binary plants generating power from low-temperature geothermal fluids, *Geothermics*, Vol. 33, 2004, pp. 565-586.

[15] Azzolin, M., Bortolin, S. and Del Col, D., Flow boiling heat transfer of a zeotropic binary mixture of new refrigerants inside a single microchannel, *International Journal of Thermal Sciences*, Vol. 110, 2016, pp. 83-95.